Phenomenological Potentials and the D$(n,p)2n$ Reaction*

D. R. KOEHLER
Army Missile Command, Redstone Arsenal, Alabama

AND

R. A. MANN
University of Alabama, Tuscaloosa, Alabama

(Received 20 January 1964)

The D$(n,p)2n$ reaction is treated in a direct interaction framework wherein the phenomenological nucleon-nucleon potentials of Gammel and Thaler are used to describe the perturbation interactions. Tensor forces as well as central forces are included and final-state interactions among the particles is considered. The final state is pictured as a continuum deuteron plus free neutron or as a continuum dineutron plus free proton. To the extent that this picture is accurate it is found that the main contributions to the cross section are supplied by the doublet to doublet transitions. The calculations furthermore suggest a "best choice" for the triplet—even parity—central potential. A comparison with the experimental results of Ilakovac and co-workers at 14.4 MeV is presented.

I. INTRODUCTION

IN many nuclear reaction processes a non-negligible contribution is accrued through a direct phenomenon in which the incident nucleon interacts with one, or at least very few, of the nucleons in the target nucleus. The reaction proceeds before the energy can be shared among a large number of particles and consequently the dynamics of the entrance channel become pertinent to the reaction description. To more adequately describe such a nuclear reaction mechanism then, direct interaction models have recently been utilized, and with modest success, for example, in stripping reactions. Some theoretical calculations have been made for direct interaction single-particle emission processes but to date little has been done on multiple-particle reactions.

One of the simpler of such multiple-particle emission processes, which has been studied by several authors,[1–4] is the D$(n,2n)p$ reaction occurring for neutrons of energy greater than 3.339 MeV. Komarov and Popova[5] have treated the mirror process D$(p,2p)n$, which with the exception of the Coulomb forces is essentially the same reaction. In that process the experimental data have prompted considerations of final-state interactions between the two protons as well as between the neutron and proton. Later work by Ilakovac, Kuo *et al.*[6,7] has shown that analogous considerations have to be made for the D$(n,2n)p$ reaction. These people, in like fashion to Komarov and Popova, work with a delta function-perturbation potential and a square-well interaction for final-state wave-function computations. In the present work, we will calculate the reaction cross section by employing the phenomenological nucleon-nucleon potentials of Gammel and Thaler[8] to represent the perturbation interaction and also to derive the final-state deuteron and dineutron wave functions. The deuteron and dineutron are spoken of in the continuum sense and are intended to describe the final-state interactions mentioned above.

In speaking of a perturbation interaction we are utilizing direct reaction theory in which context the Born approximation is used; the particle-particle interaction is treated as a perturbation on the system of nucleus plus free nucleon and it is this interaction that causes the transition, or nuclear reaction. The Born approximation has been used by others[1–5] and its justification[9] in this energy region and for this type process seems not too unreasonable. For the general case of a target nucleus consisting of A nucleons a more accurate treatment of the incoming nucleon includes a distortion of the plane wave representing the motion of the incident nucleon. This distorted wave is usually calculated with an optical potential to depict the influence of the total nuclear field on the extra nucleon. Here, however, the potential describing the cumulative effect of all the nucleons present in the target nucleus is merely $V_{nn}(|\mathbf{r}_1-\mathbf{r}_3|)+V_{np}(|\mathbf{r}_2-\mathbf{r}_3|)$, which is just the perturbation potential. A distorted (incident) wave calculation would therefore be superfluous.

From standard perturbation theory the expression for the differential cross section for transitions into the continuum is

$$d\sigma=(2\pi/\hbar v)|H_{fi}|^2\rho(E_f), \tag{1}$$

where v is the velocity of the incident nucleon, $\rho(E_f)$ is the density of final states, and H_{fi} is the matrix element between initial and final states, or transition amplitude;

$$H_{fi}=\int_\tau \phi_{\text{final}}{}^* V_{\text{interaction}}\phi_{\text{initial}}d\tau. \tag{2}$$

* Submitted in partial fulfillment of the requirements for the PhD degree at the University of Alabama.

[1] T. Y. Wu and J. Ashkin, Phys. Rev. **73**, 986 (1948).

[2] F. de Hoffmann, Phys. Rev. **78**, 216 (1950).

[3] R. L. Gluckstern and H. A. Bethe, Phys. Rev. **81**, 761 (1951).

[4] R. M. Frank and J. L. Gammel, Phys. Rev. **93**, 463 (1954).

[5] V. V. Komarov and A. M. Popova, Zh. Eksperim. i Teor. Fiz. **38**, 1559 (1960) [English transl.: Soviet Phys.—JETP **11**, 1123 (1960)].

[6] K. Ilakovac, L. G. Kuo, M. Petravic, I. Slaus, and P. Tomas, Phys. Rev. Letters **6**, 356 (1961).

[7] K. Ilakovac, L. G. Kuo, M. Petravic, and I. Slaus, Phys. Rev. **124**, 1923 (1961).

[8] J. L. Gammel and R. M. Thaler, Progr. Elem. Particle Cosmic Ray Phys. **5**, 99 (1960).

[9] W. Tobocman, *Theory of Direct Nuclear Interactions* (Oxford University Press, London, 1961).

The coordinate system and Hamiltonian description are essentially those of Bethe and Gluckstern.[3] From an interpretation of the final state as a continuum deuteron plus free neutron or as a continuum dineutron plus free proton we will write the transition amplitude as a sum of the (n,p) amplitude and the (n,n') amplitude. In other words, the reaction process is viewed as progressing through both an (n,p) mode and an (n,n') mode.

II. POTENTIALS AND WAVE FUNCTIONS

For the energy range to be considered here we will make the calculations assuming $l=0$. The choice of the phenomenological potentials of Gammel and Thaler to describe the interactions V_{nn} and V_{np} may seem somewhat arbitrary in view of the several other (e.g., Ref. 10) descriptions of nucleon-nucleon forces; however, arguments for the selection of one potential description over another are not impelling. It was felt that the G-T potentials were a satisfactory description, although Gammel and Thaler point out that the status of the n-p interaction is not satisfactory. These potentials are spin-dependent, parity-dependent, of Yukawa shape, and possess a hard core. With the assumption $l=0$ we will be interested only in the even parity components which are listed in Table I. The original work lists several possibilities for the triplet interaction, three of which are given here.

The ground-state deuteron wave function has been chosen disregarding the tensor force contribution and is of the Hulthèn type, that is

$$\Psi_0(r)=N[\exp(-\alpha r)/r](1-\exp[-\mu_c(r-r_0)]), \quad (3)$$

where

$$N=\exp(\alpha r_0)\left[\frac{2\alpha(\alpha+\mu_c)(2\alpha+\mu_c)}{4\pi\mu_c^2}\right]^{1/2},$$
$$\alpha=(ME_b/\hbar^2)^{1/2}, \quad E_b=2.226 \text{ MeV}, \quad (4)$$
$$\mu_c=\mu_c \text{ from Table I},$$

and $r_0=0.4(10)^{-13}$ cm. In the description of the final-state continuum deuteron and continuum dineutron the radial wave function is a numerical solution of the equation

$$\left(\frac{d^2}{dy^2}+k^2+b[\exp(-\mu y)/\mu y]\right)\phi_0(y)=0 \quad (5)$$

in which the potential $b\exp(-\mu y)/\mu y$ is the appropriate G-T central component. For the final state we use

$$\Psi_{\text{final}}=L^{-3/2}\{\exp(i\mathbf{k}'\cdot\mathbf{x})\Psi_{k''}(\mathbf{r})\}$$

or (6)

$$\Psi_{\text{final}}=L^{-3/2}\{\exp[i\mathbf{k}'''\cdot(-\tfrac{3}{4}\mathbf{r}-\mathbf{x}/2)]\Psi_{k^{\text{iv}}}(\mathbf{x}-\mathbf{r}/2)\},$$

which is the description referred to earlier, that of a continuum deuteron plus free neutron and a continuum dineutron plus free proton. The Ψ's result from an expansion in partial waves, that is

$$\Psi=\sum_{l=0}^{\infty}\frac{A_l\phi_l(y)}{y}P_l(\cos\theta). \quad (7)$$

This expression becomes

$$\Psi=A_0\phi_0(y)/y \text{ with the restriction } l=0. \quad (8)$$

We also subject ϕ_0 to the boundary conditions

$$\phi=0 \quad \text{at} \quad y=r_0$$

and

$$\phi=\sin(ky+\eta) \quad \text{at} \quad y=\infty.$$

By requiring that Ψ asymptotically approach the wave function describing an incident plane wave and a scattered spherical wave we get $A_0=\exp(i\eta)/k$.

Since the continuum deuteron can be either in a singlet or triplet spin state we have $\Psi_{k''^t}$, the triplet state, and $\Psi_{k''^s}$, the singlet state. For the dineutron we have only $\Psi_{k^{\text{iv}s}}$, the singlet state. The momentum notations are $\hbar\mathbf{k}''$, $\hbar\mathbf{k}'''$, and $\hbar\mathbf{k}^{\text{iv}}$, which are conjugate to the coordinates $\mathbf{r}$, $-\frac{3}{4}\mathbf{r}-\mathbf{x}/2$, and $\mathbf{x}-\mathbf{r}/2$, respectively (see Fig. 2 for further explanation of $\mathbf{k}$'s).

The spin portion of the wave function can be calculated with the help of the Clebsch-Gordan coefficients. In a representation in which σ_z is diagonal, the spin-$\frac{1}{2}$ eigenfunctions are

$$a_i\equiv\chi_{1/2}^{1/2}(i)=\begin{pmatrix}1\\0\end{pmatrix}$$

and (9)

$$b_i\equiv\chi_{1/2}^{-1/2}(i)=\begin{pmatrix}0\\1\end{pmatrix}.$$

For the initial state it is best to couple first the spins of particles 1 and 2 in the deuteron and then couple the resultant angular momentum to the spin of the neutron. Consequently for the deuteron

$$\chi_I^m(1,2)=\sum_s C(\tfrac{1}{2}\,\tfrac{1}{2}I;s,m-s)\chi_{1/2}^s(1)\chi_{1/2}^{m-s}(2), \quad (10)$$

and for the deuteron-neutron system,

$$\chi_J^M=\sum_{m_1} C(\tfrac{1}{2}IJ;m_1,M-m_1)\chi_{1/2}^{m_1}(3)\chi_I^{M-m_1}(1,2). \quad (11)$$

TABLE I. Potentials. Triplet even-parity potentials which fit the binding energy and electric quadrupole moment of the deuteron [and scattering length ${}^3a=5.39(10)^{-13}$ cm] and singlet even parity potential which fits a singlet scattering length of about $-23.74(10)^{-13}$ cm and a singlet effective range of about $2.65(10)^{-13}$ cm.

r_c^+ (10^{-13} cm)	V_c^+ (MeV)	μ_c^+ (10^{13} cm^{-1})	V_t^+ (MeV)	μ_t^+ (10^{13} cm^{-1})
		Triplet		
0.4	87.724	1.2183	272.87	1.2183
	726.69	1.9554	121.04	0.97772
	1593.5	2.2754	52.435	0.75847
		Singlet		
0.4	434.8	1.45		

[10] T. Y. Wu and T. Ohmura, *Quantum Theory of Scattering* (Prentice-Hall, Inc., Engelwood Cliffs, New Jersey, 1962).

TABLE II. Spin+space wave-function combinations.[a]

	Ψ(deuteron)			Ψ(dineutron)		
	Magnetic substate	Spin function	Space function	Magnetic substate	Spin function	Space function
$J=\frac{3}{2}$;	$m_j=\frac{3}{2}$	χ_1		$m_j=\frac{3}{2}$	χ_1	Ψ^t(din)
for $I=1$	$m_j=\frac{1}{2}$	χ_2		$m_j=\frac{1}{2}$	χ_2	
or $I'=1$	$m_j=-\frac{1}{2}$	χ_3	Ψ^t(d)	$m_j=-\frac{1}{2}$	χ_3	
	$m_j=-\frac{3}{2}$	χ_4		$m_j=-\frac{3}{2}$	χ_4	
$J=\frac{1}{2}$;	$m_j=\frac{1}{2}$	χ_5		$m_j=\frac{1}{2}$	χ_5'	
for $I=1$	$m_j=-\frac{1}{2}$	χ_6	Ψ^t(d)	$m_j=-\frac{1}{2}$	χ_6'	Ψ^t(din)
or $I'=1$						
$J=\frac{1}{2}$;	$m_j=\frac{1}{2}$	χ_7	Ψ^s(d)	$m_j=\frac{1}{2}$	χ_7'	Ψ^s(din)
for $I'=0$	$m_j=-\frac{1}{2}$	χ_8		$m_j=-\frac{1}{2}$	χ_8'	

[a] The superscript on the space wave functions denotes the singlet, s, or the triplet, t, combination of the two nucleons in the two-body particle.

This leads to a set of spin functions $\chi_i(i=1-8)$ of which four are quartet states, two correspond to an $I=1$ deuteron coupled to a spin $\frac{1}{2}$ neutron to give a $J=\frac{1}{2}$ state, and two states correspond to an $I=0$ deuteron coupled to a spin-$\frac{1}{2}$ neutron.

To explicitly display the symmetry or angular momentum coupling of particles 1 and 3, we first couple the spins of particles 1 and 3 and then couple the resultant to the spin of particle 2.

III. CROSS SECTION

We shall be considering transitions between states of sharp angular momentum of the "composite" nuclei, here the two-particle nuclei; in the initial state the deuteron and in the final state a deuteron and also a dineutron. Not only does the $I=1$ to $I'=1$ (I or I' is the angular momentum of the two-body particle) transition lead to the reaction we are considering but also the $I=1$ to $I'=0$ transition. The cross section therefore consists of two parts;

$$d\sigma=d\sigma(I=1,I'=1)+d\sigma(I=1,I'=0). \quad (12)$$

In other words, the spin of the two-body particle is treated as a good quantum number and therefore the $I=1$ to $I'=1$ and $I=1$ to $I'=0$ transition rates are computed incoherently. Since we will not be observing magnetic substates and since we will be working with a statistical distribution of spin orientations in the initial state we must average over initial spin directions and sum over the final spin states.

In Table II we have delineated the spin and space functions to be associated with the particular substates indicated in the cross section expression.

Since, as was mentioned earlier, no triplet dineutron states exist, $d\sigma(1,1)$ contains for the final state only $\Psi^t{}_{\text{deuteron}}$. From Eq. (2),

$$\begin{aligned}H_{fi}=&\int_\tau \phi_f{}^* V_{\text{int}}\phi_i d\tau\\ =&\langle(1/\sqrt{2})(1-P_{13}Q_{13})\Psi_f\chi_f|\,V_{nn}(|\mathbf{r}_{13}|)|\\ &\times(1/\sqrt{2})(1-P_{13}Q_{13})\Psi_i\chi_i\rangle\\ &+\langle(1/\sqrt{2})(1-P_{13}Q_{13})\Psi_f\chi_f|\,V_{np}(|\mathbf{r}_{23}|)|\\ &\times(1/\sqrt{2})(1-P_{13}Q_{13})\Psi_i\chi_i\rangle. \quad (13)\end{aligned}$$

The operator $(1/\sqrt{2})(1-P_{13}Q_{13})$ antisymmetrizes the wave function to account for the indistinguishability of the two neutrons. The operator P_{13} permutes the space coordinates and Q_{13} the spin coordinates of the neutrons 1 and 3. As pointed out by Bethe and Gluckstern the perturbation V must be the interaction between the particle described as free in Ψ_i, or $P_{13}\Psi_i$, and the other two. This yields

$$\begin{aligned}H_{fi}=&\langle(1/\sqrt{2})(1-P_{13}Q_{13})\Psi_f\chi_f|\,(1/\sqrt{2})(1-P_{13}Q_{13})\\ &\times[V_{nn}(|\mathbf{r}_{13}|)+V_{np}(|\mathbf{r}_{23}|)]|\Psi_i\chi_i\rangle\\ =&\langle(1-P_{13}Q_{13})\Psi_f\chi_f|\,V_{nn}(|\mathbf{r}_{13}|)\\ &+V_{np}(|\mathbf{r}_{23}|)|\Psi_i\chi_i\rangle, \quad (14)\end{aligned}$$

since $(1-P_{13}Q_{13})$ is Hermitian and $(1-P_{13}Q_{13})^2=2(1-P_{13}Q_{13})$.

The perturbation potentials V_{nn} and V_{np} are dependent on the spin states of particles 1 and 3 and particles 2 and 3. The χ_i will therefore have to be expanded to display the requisite spin orientations. For $i=1$ to 4, for example, all pairs of particles are in triplet states. This means that only the triplet component of the perturbation potential will be effective in these spin states. The two sets of spin functions mentioned earlier explicitly show the spin coupling of particles 1 and 2 and of particles 1 and 3. In a similar fashion one can construct another set to explicitly display the spin coupling of particles 2 and 3. The spin functions in any set can then be expanded in terms of the spin functions in any other set. This expansion allows one to associate the correct perturbation potential with its component in the wave function.

Neglecting, for the moment, the tensor force and performing the spin sums we get

$$\begin{aligned}d\sigma\propto&\tfrac{2}{3}|\langle(1-P_{13})\Psi_{k''}{}^{t*}(\mathbf{r})\exp(-i\mathbf{k}'\cdot\mathbf{x})|\,{}^3V_{np}(|\mathbf{x}+\mathbf{r}/2|)|\Psi_0(r)\exp(i\mathbf{k}\cdot\mathbf{x})\rangle|^2+\tfrac{1}{3}|\langle\Psi_{k''}{}^{t*}(\mathbf{r})\exp(-i\mathbf{k}'\cdot\mathbf{x})|\,{}_1U_{nn}\\ &+{}_1U_{np}|\Psi_0(r)\exp(i\mathbf{k}\cdot\mathbf{x})\rangle-\langle P_{13}\Psi_{k''}{}^{t*}(\mathbf{r})\exp(-i\mathbf{k}'\cdot\mathbf{x})|\,-{}_1U_{nn}+{}_2U_{np}|\Psi_0(r)\exp(i\mathbf{k}\cdot\mathbf{x})\rangle|^2\\ &+\tfrac{1}{3}|\langle\psi_{k''}{}^{s*}(\mathbf{r})\exp(-i\mathbf{k}'\cdot\mathbf{x})|\,{}_2U_{nn}+{}_3U_{np}|\psi_0(r)\exp(i\mathbf{k}\cdot\mathbf{x})\rangle-\langle P_{13}\psi_{k''}{}^{s*}(\mathbf{r})\exp(-i\mathbf{k}'\cdot\mathbf{x})|\,-{}_2U_{nn}\\ &+{}_4U_{np}|\psi_0(r)\exp(i\mathbf{k}\cdot\mathbf{x})\rangle+\langle\psi_k{}^{\text{iv}s*}(\mathbf{x}-\mathbf{r}/2)\exp(i\mathbf{k}'''\cdot[\tfrac{3}{4}\mathbf{r}+\mathbf{x}/2])|\,{}_3U_{nn}+{}_5U_{np}|\psi_0(r)\exp(i\mathbf{k}\cdot\mathbf{x})\rangle\\ &-\langle P_{13}\psi_k{}^{\text{iv}s*}(\mathbf{x}-\mathbf{r}/2)\exp(i\mathbf{k}'''\cdot[\tfrac{3}{4}\mathbf{r}+\mathbf{x}/2])|\,-{}_3U_{nn}-{}_5U_{np}|\psi_0(r)\exp(i\mathbf{k}\cdot\mathbf{x})\rangle|^2, \quad (15)\end{aligned}$$

where

$$\begin{aligned}
&{}_1U_{nn}=\tfrac{3}{4}\,{}^1V_{nn}(|\mathbf{x}-\mathbf{r}/2|), && {}_3U_{nn}=-\sqrt{3}/2\,{}^1V_{nn}(|\mathbf{x}-\mathbf{r}/2|),\\
&{}_1U_{np}=\tfrac{3}{4}\,{}^1V_{np}(|\mathbf{x}+\mathbf{r}/2|)+\tfrac{1}{4}\,{}^3V_{np}(|\mathbf{x}+\mathbf{r}/2|), && {}_3U_{np}=\sqrt{3}/4({}^3V_{np}(|\mathbf{x}+\mathbf{r}/2|)-{}^1V_{np}(|\mathbf{x}+\mathbf{r}/2|)),\\
&{}_2U_{nn}=\sqrt{3}/4\,{}^1V_{nn}(|\mathbf{x}-\mathbf{r}/2|), && {}_4U_{np}=-\sqrt{3}/2\,{}^1V_{np}(|\mathbf{x}+\mathbf{r}/2|),\\
&{}_2U_{np}=-\tfrac{1}{2}\,{}^3V_{np}(|\mathbf{x}+\mathbf{r}/2|), && {}_5U_{np}=-\sqrt{3}/4({}^3V_{np}(|\mathbf{x}+\mathbf{r}/2|)+{}^1V_{np}(|\mathbf{x}+\mathbf{r}/2|)).
\end{aligned} \tag{16}$$

Performing the indicated permutations we get

$$d\sigma\propto\tfrac{2}{3}|I_1-I_2|^2+\tfrac{1}{3}|\tfrac{1}{4}I_1+\tfrac{1}{2}I_2+\tfrac{3}{4}I_3+\tfrac{3}{4}I_7+\tfrac{3}{4}I_{11}|^2+\tfrac{1}{3}|(\sqrt{3}/2)(\tfrac{1}{2}I_5-2I_4+\tfrac{1}{2}I_6+\tfrac{1}{2}I_8-I_9+I_{10})|^2, \tag{17}$$

where

$$\begin{aligned}
I_1&=\int\psi_{k''}{}^{t*}(\mathbf{r})\exp(-i\mathbf{k}'\cdot\mathbf{x})\,{}^3V_{np}(|\mathbf{x}+\mathbf{r}/2|)[\psi_0(r)\exp(i\mathbf{k}\cdot\mathbf{x})]\mathbf{drdx},\\
I_2&=\int\psi_{k''}{}^{t*}(\mathbf{x}+\mathbf{r}/2)\exp(-i\mathbf{k}'\cdot[\tfrac{3}{4}\mathbf{r}-\mathbf{x}/2])\,{}^3V_{np}(|\mathbf{x}+\mathbf{r}/2|)[\psi_0(r)\exp(i\mathbf{k}\cdot\mathbf{x})]\mathbf{drdx},\\
I_3&=\int\psi_{k''}{}^{t*}(\mathbf{x}+\mathbf{r}/2)\exp(-i\mathbf{k}'\cdot[\tfrac{3}{4}\mathbf{r}-\mathbf{x}/2])\,{}^1V_{nn}(|\mathbf{x}-\mathbf{r}/2|)[\psi_0(r)\exp(i\mathbf{k}\cdot\mathbf{x})]\mathbf{drdx},\\
I_4&=\int\psi_{k^{\mathrm{iv}}}{}^{s*}(\mathbf{x}-\mathbf{r}/2)\exp(i\mathbf{k}'''\cdot[\tfrac{3}{4}\mathbf{r}+\mathbf{x}/2])\,{}^1V_{nn}(|\mathbf{x}-\mathbf{r}/2|)[\psi_0(r)\exp(i\mathbf{k}\cdot\mathbf{x})]\mathbf{drdx},\\
I_5&=\int\psi_{k''}{}^{s*}(\mathbf{r})\exp(-i\mathbf{k}'\cdot\mathbf{x})\,{}^1V_{nn}(|\mathbf{x}-\mathbf{r}/2|)[\psi_0(r)\exp(i\mathbf{k}\cdot\mathbf{x})]\mathbf{drdx},\\
I_6&=\int\psi_{k''}{}^{s*}(\mathbf{x}+\mathbf{r}/2)\exp(-i\mathbf{k}'\cdot[\tfrac{3}{4}\mathbf{r}-\mathbf{x}/2])\,{}^1V_{nn}(|\mathbf{x}-\mathbf{r}/2|)[\psi_0(r)\exp(i\mathbf{k}\cdot\mathbf{x})]\mathbf{drdx},\\
I_7&=\int\psi_{k''}{}^{t*}(\mathbf{r})\exp(-i\mathbf{k}'\cdot\mathbf{x})\,{}^1V_{np}(|\mathbf{x}+\mathbf{r}/2|)[\psi_0(r)\exp(i\mathbf{k}\cdot\mathbf{x})]\mathbf{drdx},\\
I_8&=\int\psi_{k''}{}^{s*}(\mathbf{r})\exp(-i\mathbf{k}'\cdot\mathbf{x})[{}^3V_{np}(|\mathbf{x}+\mathbf{r}/2|)-{}^1V_{np}(|\mathbf{x}+\mathbf{r}/2|)][\psi_0(r)\exp(i\mathbf{k}\cdot\mathbf{x})]\mathbf{drdx},\\
I_9&=\int\psi_{k^{\mathrm{iv}}}{}^{s*}(\mathbf{x}-\mathbf{r}/2)\exp(i\mathbf{k}'''\cdot[\tfrac{3}{4}\mathbf{r}+\mathbf{x}/2])[{}^3V_{np}(|\mathbf{x}+\mathbf{r}/2|)+{}^1V_{np}(|\mathbf{x}+\mathbf{r}/2|)][\psi_0(r)\exp(i\mathbf{k}\cdot\mathbf{x})]\mathbf{drdx},\\
I_{10}&=\int\psi_{k''}{}^{s*}(\mathbf{x}+\mathbf{r}/2)\exp(-i\mathbf{k}'\cdot[\tfrac{3}{4}\mathbf{r}-\mathbf{x}/2])\,{}^1V_{np}(|\mathbf{x}+\mathbf{r}/2|)[\psi_0(r)\exp(i\mathbf{k}\cdot\mathbf{x})]\mathbf{drdx},
\end{aligned} \tag{18}$$

and

$$I_{11}=\int\psi_{k''}{}^{t*}(\mathbf{r})\exp(-i\mathbf{k}'\cdot\mathbf{x})\,{}^1V_{nn}(|\mathbf{x}-\mathbf{r}/2|)[\psi_0(r)\exp(i\mathbf{k}\cdot\mathbf{x})]\mathbf{drdx}.$$

In I_1, I_2, I_7, I_8, I_{10}, and I_{11} one can make the substitution $\mathbf{r}=\mathbf{r}$ and $\mathbf{x}+\mathbf{r}/2=\mathbf{y}$, the Jacobian of this transformation being unity. In I_4 and I_5 one can make the transformation $\mathbf{r}=\mathbf{r}$ and $\mathbf{x}-\mathbf{r}/2=\mathbf{y}$, the Jacobian again being unity. These transformations allow one to integrate over angles and over one of the radial variables and we are left with a single radial integral in y or r. This remaining radial integration was performed numerically on the IBM-7094 computer (see Appendix). A transformation does not simplify the integrals I_3, I_6, or I_9, and these integrations were likewise done numerically. The limits on the radial integration are from r_0, the radius of the hard core, to ∞.

Let us now consider the tensor force contribution to the cross section. We have

$${}^3V={}^3V_{np}=({}^3V_{np})_{\text{central}}+({}^3V_{np})_{\text{tensor}}, \tag{19}$$

where

$$({}^3V_{np})_{\text{tensor}}=-{}^3V_t[\exp(-\mu_t r)/\mu_t r]S_{ij} \tag{20}$$

and where i, j denote the interacting particles (2 and 3

in our notation). Also

$$S_{ij}=S_{23}=3(\boldsymbol{\sigma}_2\cdot\mathbf{n})(\boldsymbol{\sigma}_3\cdot\mathbf{n})-(\boldsymbol{\sigma}_2\cdot\boldsymbol{\sigma}_3),$$

where $\mathbf{n}$ is the unit vector along the line joining the two particles. In the spin representation chosen here σ_z is diagonal. If we choose the vector direction $\mathbf{q}$ ($\mathbf{q}=\mathbf{k}'-\mathbf{k}$) as the polar or Z axis, we have the coordinate system displayed in Fig. 1.

Whereas with the central force the off-diagonal elements were zero (i.e., m quantum number conserved) we now get a finite contribution to the cross section from some of them. Upon calculating the tensor force-matrix elements it is found that the only nonzero terms appear in $d\sigma$ (quartet). Since interference terms between central and tensor forces are proportional to the trace of S_{ij} (in spin space) and since this trace is zero, the tensor force components are incoherent with the central force elements.

In general, the tensor force induces quartet to doublet and doublet to quartet transitions as well as quartet to quartet transitions. However, doublet to doublet transitions do not occur. This latter statement can be verified by direct calculation but can also be proved in the following manner: The tensor force can be written as a scalar product of a tensor operator of rank two (operating in spin space) and the spherical harmonic of second degree.[11] Applying the Wigner-Eckart theorem[12] to matrix elements involving such an operator we get

$$\langle j'm'|T_{LM}|jm\rangle=C(jLj';mMm')\langle j\|T_L\|j'\rangle. \quad (21)$$

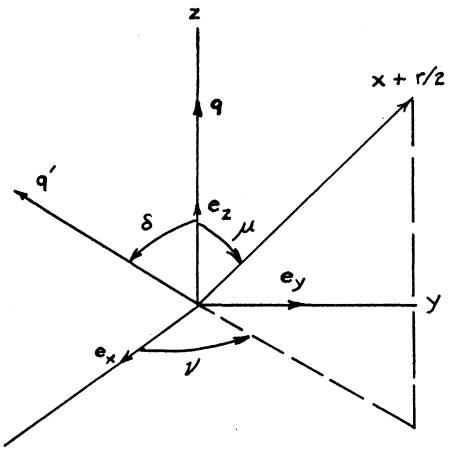

FIG. 1. Coordinate system for tensor force integrations.

This C coefficient vanishes unless the triangle condition $\Delta(jLj')$ holds; i.e., $C(\frac{1}{2}2\frac{1}{2};mMm')=0$. For $J=\frac{1}{2}$, then J' must equal $\frac{5}{2}$ or $\frac{3}{2}$. Since we are here considering $l=0$, total angular momentum conservation forbids the quartet-doublet and doublet-quartet transitions. We are left then with only the quartet-quartet transitions and

$$d\sigma_{\text{tensor}}\propto\frac{2J+1}{2(2I+1)}\left(\frac{1}{2J+1}\sum_{m_j}\right)\sum_{m_{j'}}|H_{fi}|^2. \quad (22)$$

Thus, after performing the indicated spin sums,

$$\begin{aligned}d\sigma_{\text{tensor}}\propto\tfrac{2}{3}\times\tfrac{1}{4}\times\{&4|\langle(1-P_{13})\Psi_f\,{}^3V_{np}{}^{\text{tensor}}(|\mathbf{x}+\mathbf{r}/2|)[3\cos^2\mu-1]\Psi_i\rangle|^2\\&+2|\langle(1-P_{13})\Psi_f\,{}^3V_{np}{}^{\text{tensor}}(|\mathbf{x}+\mathbf{r}/2|)[\exp(2i\nu)\sqrt{3}\sin^2\mu]\Psi_i\rangle|^2\\&+2|\langle(1-P_{13})\Psi_f\,{}^3V_{np}{}^{\text{tensor}}(|\mathbf{x}+\mathbf{r}/2|)[\exp(-2i\nu)\sqrt{3}\sin^2\mu]\Psi_i\rangle|^2\\&+2|\langle(1-P_{13})\Psi_f\,{}^3V_{np}{}^{\text{tensor}}(|\mathbf{x}+\mathbf{r}/2|)[\exp(i\nu)2\sqrt{3}\sin\mu\cos\mu]\Psi_i\rangle|^2\\&+2|\langle(1-P_{13})\Psi_f\,{}^3V_{np}{}^{\text{tensor}}(|\mathbf{x}+\mathbf{r}/2|)[\exp(-i\nu)2\sqrt{3}\sin\mu\cos\mu]\Psi_i\rangle|^2\}. \quad (23)\end{aligned}$$

After making the change of variable $\mathbf{r}=\mathbf{r}$ and $\mathbf{x}+\mathbf{r}/2=\mathbf{y}$ the direct integrals in the last four elements vanish in the integration over the azimuthal angle ν. To incorporate further the approximation that we are concerned only with s-wave encounters, we now need to expand the plane wave functions in a Rayleigh expansion. For example,

$$\exp(i\mathbf{q}\cdot\mathbf{y})=\sum_{l=0}^{\infty}(i)^l(2l+1)P_l(\cos\theta)j_l(qy),$$

where θ is the angle between $\mathbf{q}$ and $\mathbf{y}$, $P_l(\cos\theta)$ is the Legendre polynomial, and $j_l(qy)$ is the spherical Bessel function. This plane wave becomes, in our approximation,

$$\exp(i\mathbf{q}\cdot\mathbf{y})\approx\sin qy/qy;$$

comparable substitutions are made for the other plane-wave functions. Now in similar fashion with the direct integrals the exchange integrals in the last four elements vanish in the integration over the azimuthal angle ν. The other integrals vanish in the integration over μ. Thus $d\sigma_{\text{tensor}}=0$.

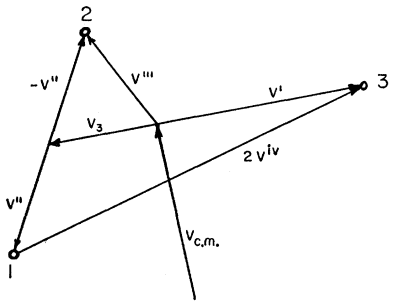

FIG. 2. Velocity vector diagram.

[11] M. Verde, in *Handbuch der Physik*, edited by S. Flügge (Springer-Verlag, Berlin, 1957), Vol. 39, p. 164.

[12] M. E. Rose, *Elementary Theory of Angular Momentum* (John Wiley & Sons, Inc., New York, 1957).

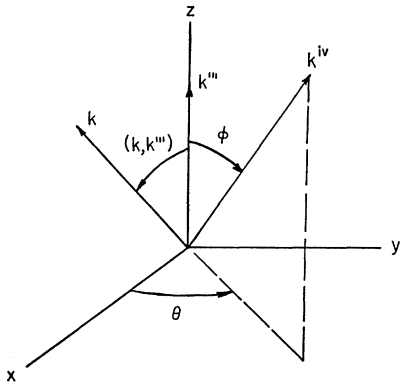

FIG. 3. Coordinate system for integration over $d\Omega^{iv}$.

Referring now to Eq. (1), let us rewrite the cross section formula to allow a comparison with the experimental data. We have

$$\rho(E_f)dE_f=\frac{\mathbf{dp}'''}{h^3}\times\frac{\mathbf{dp}^{iv}}{h^3}=\frac{\mathbf{dk}'''\mathbf{dk}^{iv}}{(2\pi)^6}. \tag{24}$$

We will be calculating an energy spectrum of the emitted protons and thus the use of $\mathbf{k}'''$, the wave vector for the proton. In observing the proton we will be fixing the angle and energy, i.e., fixed $\mathbf{k}'''$; the magnitude of $\mathbf{k}^{iv}$ is determined from the energy equation and the remaining degrees of freedom (direction of $\mathbf{k}^{iv}$) are removed by integrating over $d\Omega^{iv}$. We can write therefore

$$\rho(E_f)=(k^{iv})^2d\Omega^{iv}(\partial k^{iv}/\partial E_f)_{\mathbf{k}'''}[\mathbf{dk}'''/(2\pi)^6], \tag{25}$$

where we can deduce

$$(\partial k^{iv}/\partial E_f)_{\mathbf{k}'''}=M/2\hbar^2k^{iv}$$

from the energy equation

$$\frac{\hbar^2(k''')^2}{\frac{4}{3}M}+\frac{\hbar^2(k^{iv})^2}{M}=E_f. \tag{26}$$

To transform to the laboratory system consider the vector diagram in Fig. 2. We let $\mathbf{v}_3$=velocity of the "deuteron" system about the c.m. and $\mathbf{v}'$=velocity of the scattered neutron about the c.m. to correspond to the earlier notation. Then $\mathbf{v}_3=-\mathbf{v}'/2$ and since $\mathbf{v}'''=\mathbf{v}_3-\mathbf{v}''$, the velocity of particle 2 in the laboratory system is

$$\mathbf{v}_{lab}=\mathbf{v}'''+\mathbf{v}_{c.m.}=\mathbf{v}_3-\mathbf{v}''+\mathbf{v}/2,$$

or

$$\mathbf{k}'''=-\mathbf{k}'/2-\mathbf{k}'', \tag{27}$$

and

$$\mathbf{k}_p=\mathbf{k}_{lab}(\text{particle 2})=-\mathbf{k}'/2-\mathbf{k}''+\mathbf{k}/2. \tag{28}$$

We also need $\mathbf{v}^{iv}$ (or $\mathbf{k}^{iv}$), but

$$2\mathbf{v}^{iv}=\mathbf{v}'-(\mathbf{v}_3+\mathbf{v}'')=\tfrac{3}{2}\mathbf{v}'-\mathbf{v}'', \tag{29}$$

or

$$\mathbf{k}^{iv}=\tfrac{3}{4}\mathbf{k}'-\tfrac{1}{2}\mathbf{k}''.$$

From these equations we can express, where necessary, $\mathbf{k}'$ and $\mathbf{k}''$ in terms of $\mathbf{k}'''$ and $\mathbf{k}^{iv}$.

Furthermore since

$$\mathbf{k}_p=\mathbf{k}'''+\mathbf{k}/2,$$
$$\mathbf{dk}_p=\mathbf{dk}'''=k_p^2dk_pd\Omega_p=k_p(M/\hbar^2)dE_pd\Omega_p. \tag{30}$$

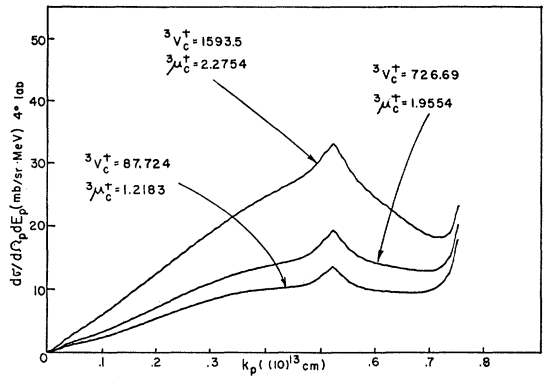

FIG. 4. Energy spectrum of protons emitted at 4° lab and comparison with experimental data.

FIG. 5. The differential cross section as a function of the triplet potential strength.

Thus the "inelastic neutron emission" cross section becomes

$$d\sigma=\frac{2\pi k^{iv}}{2\hbar}\left(\frac{2M}{3\hbar k}\right)\left(\frac{M}{2\hbar^2}\right)^2\frac{2k_pdE_pd\Omega_p}{(2\pi)^6}\int|H_{fi}|^2d\Omega^{iv}$$
$$=\frac{1}{6(2\pi)^5}\left(\frac{M}{\hbar^2}\right)^3\frac{k_pk^{iv}}{k}dE_pd\Omega_p\int|H_{fi}|^2d\Omega^{iv}, \tag{31}$$

where we have divided by a factor of 2 to account for the indistinguishability of the two neutrons. In a quantum mechanical treatment there is included in the inelastic scattering calculation those processes wherein the "target" neutron is ejected into the solid angle $d\Omega$ and so (in the strict sense of the inelastic process where the incident particle emerges with a degraded energy) we must include this factor of 2 to compensate for the fact that we have included *two* "neutron emission" possibilities. Of course experimentally, if one observes

"neutrons," one will not be able to distinguish their origin, and therefore to compare experiment with theory one needs to multiply the "inelastic neutron emission" cross section by 2. The differential cross section per unit solid angle per unit energy then becomes

$$\frac{d\sigma}{d\Omega_p dE_p}=\frac{1}{6(2\pi)^5}\left(\frac{M}{\hbar^2}\right)^3\frac{k_p k^{\mathrm{iv}}}{k}\int|H_{fi}|^2 d\Omega^{\mathrm{iv}}. \quad (32)$$

The coordinate system for the integration over $d\Omega^{\mathrm{iv}}$ is shown in Fig. 3. We want the final expression in terms of the angle between $\mathbf{k}$ and $\mathbf{k}_p$ and so use

$$\mathbf{k}\cdot\mathbf{k}'''=kk'''\cos(\mathbf{k},\mathbf{k}''')=\mathbf{k}\cdot\mathbf{k}_p-\tfrac{1}{2}(\mathbf{k}\cdot\mathbf{k}) \quad (33)$$

and

$$\cos(\mathbf{k},\mathbf{k}^{\mathrm{iv}})=\frac{\mathbf{k}\cdot\mathbf{k}^{\mathrm{iv}}}{kk^{\mathrm{iv}}}=\cos(\mathbf{k},\mathbf{k}''')\cos\phi+\sin(\mathbf{k},\mathbf{k}''')\cos\theta\sin\phi. \quad (34)$$

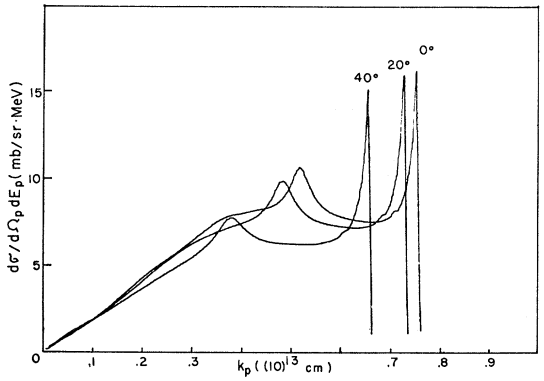

FIG. 6. The differential cross section versus angle $(\mathbf{k},\mathbf{k}_p)$.

From the energy equation we have

$$(k''')^2+\tfrac{4}{3}(k^{\mathrm{iv}})^2=k^2-\tfrac{4}{3}(M/\hbar^2)\times E_b$$

or

$$(k^{\mathrm{iv}})^2=\tfrac{3}{4}(K^2-\{k_p{}^2+k^2/4-\mathbf{k}\cdot\mathbf{k}_p\}), \quad (35)$$

where

$$K^2=k^2-\tfrac{4}{3}(M/\hbar^2)\times E_b.$$

In constructing an energy spectrum of emitted protons at a given angle $(\mathbf{k},\mathbf{k}_p)$, we let k_p vary from zero up to a maximum

$$k_p(\max)=k/2\cos(\mathbf{k},\mathbf{k}_p)+\{k^2/4\cos^2(\mathbf{k},\mathbf{k}_p)+(K^2-k^2/4)\}^{1/2} \quad (36)$$

and determine k^{iv} from Eq. (35).

IV. COMPARISON WITH EXPERIMENTAL RESULTS AND DISCUSSION

The major contributions to the cross section come from the doublet transitions, namely $d\sigma(I=1, I'=0)$ and the $J=\frac{1}{2}$ portion of $d\sigma(I=1, I'=1)$. The quartet to quartet matrix elements are smaller by at least two orders of magnitude than the doublet-doublet matrix elements, however the doublet transitions mentioned above are of the same order of magnitude. Therefore, the present treatment does not allow one to neglect the $d\sigma(I=1, I'=1)$ doublet contribution. This result is to be contrasted with the work of Komarov and Popova.[5]

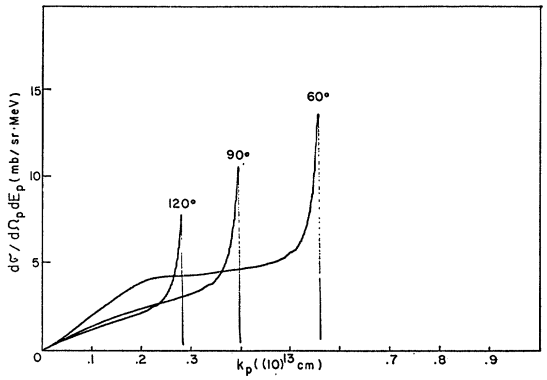

FIG. 7. The differential cross section versus angle $(\mathbf{k},\mathbf{k}_p)$.

In Fig. 4 we compare the present theoretical calculations with the experimental data of Ilakovac *et al.*[6] This figure displays the energy spectrum of protons emitted at an angle of 4° in the laboratory system and an incident neutron energy of 14.4 MeV. No attempt has been made to smear the theoretical calculations in this comparison. Figure 5 shows the dependence of the cross section calculations on the choice of triplet–even-parity–central potential. The behavior of the two peaks in the spectrum, that is their dependence on the triplet–even-parity potential, is as expected since the high-energy peak $(k^{\mathrm{iv}}=0)$ corresponds to the neutron-neutron interaction, which is singlet only, and the low-energy peak $(k''=0)$ corresponds to the interaction between neutron and proton, which is both singlet and triplet. There is some contribution to the high-energy peak from the neutron-proton interaction and thus the increase indicated in Fig. 5. It is readily seen from these results that the best agreement with the experimental data is

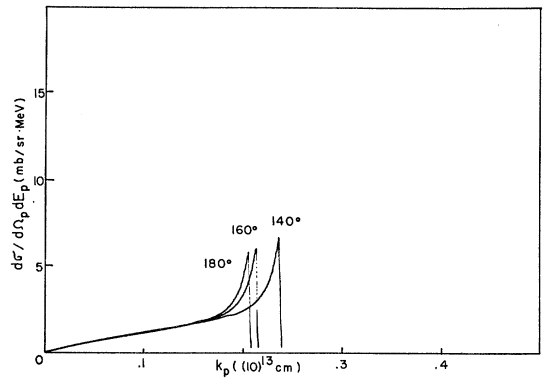

FIG. 8. The differential cross section versus angle $(\mathbf{k},\mathbf{k}_p)$.

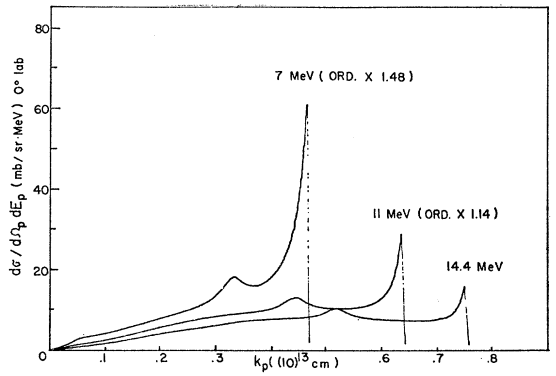

FIG. 9. The differential cross section versus incident neutron energy. The cross section (ordinate) is to be multiplied by the factor in parenthesis for each energy value.

attained with the first of the three sets in Table I, that is ${}^3V_c{}^+=87.72$ MeV and ${}^3\mu_c{}^+=1.2183\ 10^{13}$ cm^{-1}. It is to be noted that quantitative as well as qualitative agreement with experiment is achieved in the present treatment. Furthermore, the marked quantitative dependence of these calculations on the strength and range of this potential suggest the possible use of these reaction data in the phenomenological approach to the nucleon-nucleon interaction.

Proton energy spectra have been calculated at several angles and the results are shown in Figs. 6–8. These particular calculations have been performed with the above "best fit" potential parameters and at an incident neutron energy of 14.4 MeV. One observes that the high-energy proton peaking prevails in the backward directions as well. This result is in agreement with recent calculations by Ferroni and Wataghin,[13] for example, but in disagreement with the experimental results of Ref. 14.

The dependence of the cross section on the incident neutron energy is shown in Fig. 9. As the neutron energy is decreased these calculations are perhaps not expected to give good results due to the present description of the reaction mechanism. The complications of the three-body problem are more manifest when the momentum of the incoming particle is comparable to the momentum of the particles in the deuteron.

In summary the present calculations seem to give fairly good agreement with the experimental data although one needs to ascertain the effect of neglecting $l>0$ angular momentum encounters with the resulting tensor and spin-orbit contributions to the cross section.

[13] F. Ferroni and V. Wataghin, Nuovo Cimento **28**, 2888 (1963).
[14] K. Ilakovac, L. G. Kuo, M. Petravic, I. Slaus, and P. Tomas, Nucl. Phys. **43**, 254 (1963).

ACKNOWLEDGMENTS

We wish to acknowledge the help of Dr. William L. Alford in many fruitful discussions. The cooperation and assistance of the Computation Laboratory personnel in the numerical computations is also acknowledged.

APPENDIX

The problem as presented to the IBM 7094 consisted of evaluating the following expression:

$$\frac{d\sigma}{A}=2\pi k^{\mathrm{iv}}k_p\int_{\phi=0}^{\pi}H(\phi)\sin(\phi)d\phi,$$

where

$$H(\phi)=\tfrac{2}{3}(H_1)^2+\tfrac{1}{3}(H_2)^2+\tfrac{1}{4}(H_3)^2,$$

and

$$(H_1)^2=(I_1-I_2)^2,$$
$$(H_2)^2=(\tfrac{1}{4}I_1+\tfrac{3}{4}I_7+\tfrac{1}{2}I_2+\tfrac{3}{4}I_3+\tfrac{3}{4}I_{11}),$$
$$(H_3)^2=a^2+b^2-2ab\cos(\eta_2-\eta_1),$$
$$a=\tfrac{1}{2}I_5+\tfrac{1}{2}I_6+\tfrac{1}{2}I_8+I_{10},$$

and

$$b=2I_4+I_9.$$

The arguments η_1 and η_2 represent the asymptotic phases, respectively, of the singlet dineutron and singlet deuteron.

As mentioned in the text, some of the integrals are simplified by transformations and can be reduced to a single integral over a radial variable; however, I_3, I_6, and I_9 cannot be so simplified and thus require integration over the six-dimensional product space of **x** and **r**. The $l=0$ approximation is further manifested by replacing the plane wave functions by their spherically symmetric Rayleigh expansion components [$\sin(kx)/kx$, etc.], thus reducing the six-dimensional integration to a two-dimensional one.

The Runge-Kutta method was used to solve the radial part of the wave equation describing the final-state two-body particles [Eq. (5)]. The final-state wave functions and the initial-state wave functions were then tabulated as functions of their spatial arguments; for the final-state wave functions $\Psi_{k''}$ and $\Psi_{k^{\mathrm{iv}}}$, the tabulations were also made as a function of the energy parameter k''^2 and $k^{\mathrm{iv}2}$. The potential functions were similarly tabulated as functions of their spatial arguments. Thus the integrals involved products, the factors of which were all tabulated.